Chemical Physics Letters 793 (2022) 139477

Contents lists available at ScienceDirect

Chemical Physics Letters

journal homepage: www.elsevier.com/locate/cplett

Stability of hydrogenated silica glass and desorption kinetics of molecular hydrogen

K.P. Meletov *, V.S. Efimchenko

Institute of Solid State Physics, Russian Academy of Sciences, Chernogolovka, Moscow Region 142432, Russia

ARTICLE INFO

Keywords:
Hydrogen-storage solids
Hydrogen desorption
High pressure
Raman scattering

ABSTRACT

The stability of saturated solid solutions of molecular hydrogen in silica glass was examined in the temperature range 85 ÷ 175 K by Raman spectroscopy. The kinetics of hydrogen desorption was studied *in-situ* by tracking time-dependent changes in the intensities of hydrogen rotational modes at an elevated temperature. The heating results in an exponential decrease in the hydrogen content with a temperature dependent time constant. The data at different temperatures are well described by the Arrhenius formula showing the activation character of desorption with the activation energy $E_A = (0.16 \pm 0.01)$ *eV* and time constant $A = (0.027 \pm 0.003)$ sec.

1. Introduction

The uptake of hydrogen has been observed in metals and alloys, carbon nanostructures, clathrates of various gases, and ice hydrates [1–4]. Generally, a search for new hydrogen storage solids is relevant due to their ability to contain more hydrogen per unit volume, which is a good alternative to storing liquid hydrogen [5–6]. The amount of absorbed hydrogen, the availability of absorbing and releasing way, and the prevalence of the employed material are the key parameters for the applications. In view of this, a variety of silicate glasses may have the potential to be used as hydrogen storage materials. The first experiments in 1976 discovered certain solubility of hydrogen in silica glass at a temperature of 90 °C and gas pressure between 6.6 and 84.9 MPa [7]. The Raman probes of hydrogenated silica glass identified the H-H stretching vibration mode of hydrogen molecule growing in intensity with an increase in the dissolved hydrogen content to the maximum of ~0.06 H_2/SiO_2 at 84.9 MPa. The saturated solutions of hydrogen in silica glass were synthesized later at rather high hydrogen pressures and a temperature of 250 °C, the molecular ratio $X = H_2/SiO_2$ increasing from $X = 0.16$ at 0.6 GPa to $X = 0.53$ at 7.5 GPa [8]. Subsequently, the solid solutions of hydrogen were synthesized under similar conditions in some other complex silicates containing magnesium or iron cations, and the efficiency of molecular hydrogen absorption, the changes in the matrix structure and phonon spectra, as well as possible chemical reactions upon hydrogenation were studied in [9–12].

After synthesis, the samples of hydrogenated silica glass must be stored in a liquid nitrogen vessel to prevent hydrogen losses. Thus, the hydrides are unstable under ambient conditions and exhibit extensive hydrogen desorption even at rather low temperatures. The amount of dissolved hydrogen in hydrogenated materials is determined usually by hot desorption, while the appearance of hydrogen in a molecular form can be verified by Raman spectroscopy using the H-H stretching vibration mode as a fingerprint [8,9]. The hot desorption method provides accurate information on the total content of dissolved hydrogen, the approximate temperature ranges of hydride stability and hydrogen emission; however, it is not well suitable for studying the kinetics of hydrogen desorption. Alternatively, the current content of hydrogen can be estimated from the intensity of its phonon modes in the Raman spectra of hydrides relative to those of silica glass. In this way, it is possible to trace the changes in the hydrogen content *in-situ* during the annealing of hydrogenated silica glass samples under various temperature conditions.

The Raman study of the hydrogenated silica glass shows distinct changes in the intensities of H-H stretching vibration and rotational modes of hydrogen with a change in its concentration. The difference appears when the hydrogen content increases under higher synthesis pressure or decreases under the annealing of hydrogenated samples at high temperature [13]. Another type of changes in the Raman spectra of hydrides takes place with isotopic substitution of hydrogen by deuterium which results in softening of the stretching vibration and rotational modes [13]. Thus the loss of hydrogen in hydrogenated silica glass leads to a decrease in the intensity of rotational modes with respect to the total intensity of the silica glass phonon modes. These changes in the Raman spectra can be used for tracking the time-dependent changes in the

* Corresponding author.
E-mail address: mele@issp.ac.ru (K.P. Meletov).

https://doi.org/10.1016/j.cplett.2022.139477
Received 21 October 2021; Received in revised form 19 January 2022; Accepted 15 February 2022
Available online 18 February 2022

hydrogen content under annealing. Quantitative data obtained at various annealing temperatures may be very useful for the study of hydrogen desorption kinetics.

In the present work, we have studied the time evolution of the Raman spectra of various hydrogenated silica glass samples with initial hydrogen content between X = 0.58 and X = 0.7 in the temperature range 143 ÷ 190 K. The heating leads to an exponential decrease in the intensity of the rotational hydrogen modes, while the time constant of the exponential decay decreases wen the annealing temperature increases. Hydrogen desorption grows so fast with temperature that the exponential decay time constant τ decreases from 215 min at 143 K to 5.9 min at 190 K. The dependence of the time constant τ on the annealing temperature T is well described by the Arrhenius formula $\tau(T) = A*\exp(E_A/k_BT)$ showing an activating nature of desorption with the activation energy $E_A = (0.16 \pm 0.01)$ eV and $A = (0.027 \pm 0.003)$ sec. Based on the numerical data obtained, we estimated the stability of saturated solid solutions of hydrogen in silica glass; hydrogen content falls in half within ~17 years at a liquid nitrogen temperature and within 10 s under ambient conditions.

2. Experimental

The samples of OH-Vitreosil silica glass purchased from Sigma–Aldrich with 99.9 wt% purity contained <0.01 wt% metals and <0.06 wt% OH^- impurities. The initial samples were annealed before hydrogenation for 4 h at 800 °C to eliminate residual hydroxyls and water. The hydrogenation was carried out in a Toroid-type high-pressure apparatus [14] using AlH_3 [15] or NH_3BH_3 [16] as an internal hydrogen source. The high-pressure cell was made of Teflon; a Pd foil separated the hydrogen source from the silica glass. To evolve hydrogen, AlH_3 or NH_3BH_3 was decomposed at P = 1.5 GPa by heating to T = 250 °C. The pressure was then increased, and the silica glass sample was exposed to an H_2 atmosphere at P = 7.5 GPa and T = 250 °C for 24 h. Then, it was quenched in liquid nitrogen to prevent hydrogen losses in the course of the subsequent pressure release and the following long-term storage. The molar ratio $X = H_2/f.u.$ of the samples was determined with an accuracy of δX = 0.03 by hot extraction into a pre-evacuated volume [17]. The Raman spectra were recorded in backscattering geometry at near liquid nitrogen temperature and spectral range of 150–4400 cm^{-1} using a micro-Raman setup comprised of an Acton SpectraPro-2500i spectrograph and a CCD Pixis2K detector system. The 532 nm-line of a single-mode YAG CW diode-pumped laser was focused on the sample by an Olympus BX51 50× objective in a ~2-μm-diameter spot with a spectral resolution of ~3 cm^{-1}. The laser line was suppressed by an edge filter with the optical density OD = 6 and bandwidth of ~100 cm^{-1}, while the beam intensity in front of the sample was ~6 mW. The Raman measurements at various temperatures were performed using a home-made nitrogen cryostat, which permitted cold loading of the samples from liquid nitrogen into the cryostat without intermediate warming. The cryostat equipped with a temperature controller and resistive heater on the heat exchanger provided temperature control in the temperature range of 83–250 K with an accuracy of ±0.4 K [18].

3. Results and discussion

The Raman spectrum of SiO_2-0.6H_2 hydrogenated silica glass is shown in Fig. 1 in the energy range 150 ÷ 4400 cm^{-1} at T ≈ 85 K (solid line). The dashed line in the figure depicts the spectrum of silica glass measured under similar conditions before hydrogenation; it coincides in detail with the early reported phonon spectrum of pristine silica glass [19]. The spectrum of the hydrogenated sample differs greatly from that of initial silica glass due to a number of new appeared bands. The most intense new band appears at ~4190 cm^{-1} in the high-energy region of the spectrum. In addition, a rather intense band at ~328 cm^{-1} and a weaker band at ~549 cm^{-1} appear in the low-frequency region; they overlap with the phonon spectrum of silica glass. The band at ~4190 cm^{-1} corresponds to the H-H stretching vibration mode of molecular hydrogen, while the bands at ~328 cm^{-1} and ~549 cm^{-1} correspond to the rotational modes of the diatomic molecule [13]. The positions of the silica glass phonon bands in the hydride and intensity distribution between them change somewhat compared to those of pristine silica glass. The phonon peaks of hydrogenated silica glass are slightly shifted to lower energies with respect to those of pristine silica glass. The softening of the modes is rather large for acoustic phonons and smaller for optical phonons; it is related most likely to the expansion of the silica glass matrix under hydrogenation. The changes in the intensity may be associated with the local van der Waals interaction between SiO_2 and H_2 molecules located in the pores of silica glass that modifies the phonon spectrum.

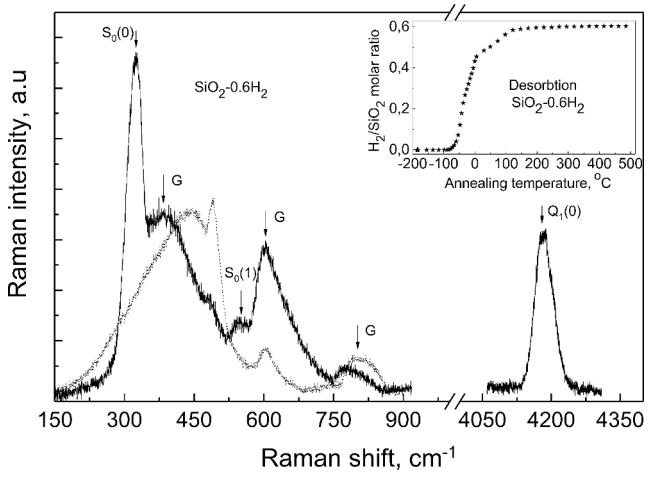

Fig. 1. Raman spectra of hydrogenated SiO_2-0.6H_2 silica glass (solid line) and pristine SiO_2 silica glass (dotted line) measured in the energy region of 150 – 4380 cm^{-1} at ambient pressure and T≈85 K. $S_0(0)$ and $S_0(1)$ – hydrogen rotational modes, $Q_1(0)$ – hydrogen stretching vibration mode, G – phonon modes of silica glass. Inset – desorption curve of hydrogen hot extraction for SiO_2-0.6H_2.

The intensity of new Raman bands grows with an increase in the hydrogen content at higher synthesis pressure but decreases upon hydrogen desorption under annealing of hydrides at elevated temperature. Annealing at room temperature is very fast and the hydrogen bands quickly disappear, while the phonon spectrum of the silica glass matrix is restored to that of pristine silica glass. The phonon bands of hydrogen in the hydrogenated silica glass are strongly broadened. The bandwidths of the stretching vibration and rotational modes are ~45 cm^{-1} and ~35 cm^{-1}, respectively, whereas their bandwidths in the Raman spectrum of gaseous hydrogen are ~3 cm^{-1}. The Raman frequencies for dissolved hydrogen differ from those of hydrogen gas: the rotational modes are shifted by ~20 cm^{-1} downward, and the stretching vibration mode is shifted by ~30 cm^{-1} upward. The intensity ratio of two rotational modes indicates the predominance of *para*-hydrogen in the silica glass hydride. Such a distribution of intensity between them is due to the storing of the hydrogenated samples in liquid nitrogen; at this temperature, *para*-hydrogen predominates because of ortho-para conversion [13,20,21]. The total content of the dissolved hydrogen in hydrides was determined by hot extraction in an evacuated vessel with a calibrated volume of 50 cm^3 under heating from 190 to 500 °C at a rate of ~15 °C /min. The hydrogen desorption curve from the SiO_2-0.6H_2 sample is shown in the inset in Fig. 1. Typically, the rate of desorption is very small at temperatures up to −100 °C, but it increases significantly at higher temperatures reaching the maximum near 0 °C. The determination of hydrogen content by hot desorption is basically used for all hydrides; however, the study of hydrogen desorption kinetics requires a different approach. We have chosen Raman spectroscopy to monitor the intensity of phonon bands of molecular hydrogen as a more suitable and fairly

accurate method for the study of hydrogen desorption in hydrogenated silica glass.

Fig. 2 depicts the Raman spectra of hydrogenated SiO_2-0.58H_2 silica glass measured in the frequency range 230 ÷ 920 cm^{-1} after 3, 10, 26 and 60 min of annealing at T = 183 K. The relative intensity of the hydrogen rotational modes in the spectra gradually decreases with an increase in the annealing time. The effect can be characterized quantitatively by the ratio of the total intensity of the hydrogen rotational modes to the total intensity of the phonon modes of silica glass, which does not change upon annealing and serves as a scale. The open circles in Fig. 2 show the experimental dependence of hydrogen content on the annealing time obtained in this way in the course of 85 min of annealing. All data are normalized to the initial value of hydrogen content X = 0.58 determined independently by hot extraction. The experimental dependence is well approximated by the exponential decay function $I_H/I_G = 0.25*\exp(-t/10.7) + 0.33$ shown in Fig. 2 with a dashed line. The time constant of the exponential decay is ~10.7 min, while the hydrogen desorption saturates at a long annealing time showing residual content of X≈0.33. In backscattering geometry, the Raman spectra are recorded from the surface of the sample due to the sharp focusing of the laser beam. Therefore, the observed decrease in the intensity of the hydrogen bands refers to desorption from the surface of the hydride. At the same time, slow diffusion of hydrogen from the depth leads to its partial replenishment. At a certain stage of annealing, the amount of hydrogen released from the sample surface is replaced by the equal amount of hydrogen incoming from the bulk due to diffusion. This steady-state can be achieved at a relatively small diffusion rate, which results in the appearance of residual hydrogen content as measured by Raman spectroscopy.

Fig. 3 illustrates the experimental data on hydrogen desorption at five different temperatures in the range 143 ÷ 190 K. Different symbols show the experimental dependence of the relative hydrogen content C_t/C_0 on the annealing time t at different temperatures. At each temperature, a new fresh sample was used for the serial measurements of Raman spectra with a fixed time interval between them. The total exposure time for each measurement was longer than the interval between them. Experimental data on hydrogen content (open symbols) show a gradual decrease with annealing time that can be fitted with the exponential decay function (dashed lines). The time constant of the exponential decay decreases from 215 min at 143 K to 5.9 min at 190 K. With a further increase in the annealing temperature, hydrogen desorption becomes so fast that reliable measurements of the Raman spectra become impossible. An increase in the annealing temperature results also in a decrease in the residual hydrogen content C_t/C_0 in the annealed

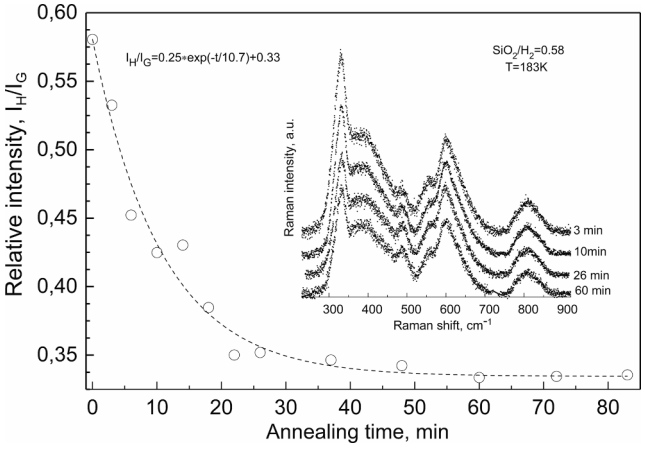

Fig. 2. Raman spectra of hydrogenated SiO_2-0.58H_2 silica glass taken at 3, 10, 26 and 60 min of annealing at 183 K. Open circles – experimental dependence of relative hydrogen content on the annealing time; dotted line – fitting by the exponential decay function.

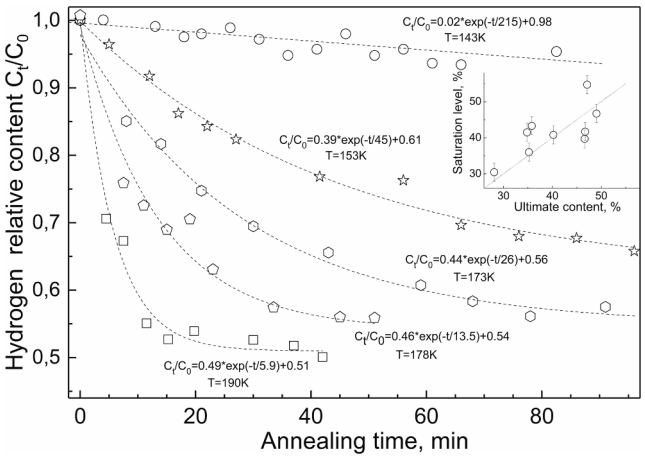

Fig. 3. Time dependence of the relative hydrogen content C_t/C_0 under annealing at 143, 153, 173, 178 and 190 K (open symbols); dashed line – fitting of the experimental data by the exponential decay function. Inset: residual hydrogen content upon long-time annealing of the hydrogenated silica glass samples versus the ultimate hydrogen content determined by hot extraction after the annealing.

samples from 0.98 at 143 K to 0.51 at 190 K. In our opinion, this follows from the competition between hydrogen desorption from the surface of the sample and more intense diffusion of hydrogen from the bulk of the sample at a higher temperature. After completing the Raman measurements at a certain temperature, some hydride samples were studied by hot extraction to independently determine the residual hydrogen content. The open circles in the inset in Fig. 3 compare the "ultimate" C_t/C_0 values obtained in this way (the X-coordinate) with those derived from the Raman spectra and used as the Y-coordinates. Rather scattered experimental data are located near the linear X = Y dependence (broken line). The observed correlation confirms a decrease in the real content of dissolved hydrogen under annealing and suggests the homogeneous distribution of H_2 molecules over the bulk and surface of the annealed samples.

The hydrogen desorption in silica glass hydrides demonstrates the activation type of behavior that is justified by the dependence of the exponential decay time constant τ on temperature T shown in Fig. 4. Irrespectively of the starting hydrogen content (X = 0.58, X = 0.6, X = 0.62, or X = 0.7), all experimental points can be well represented by the

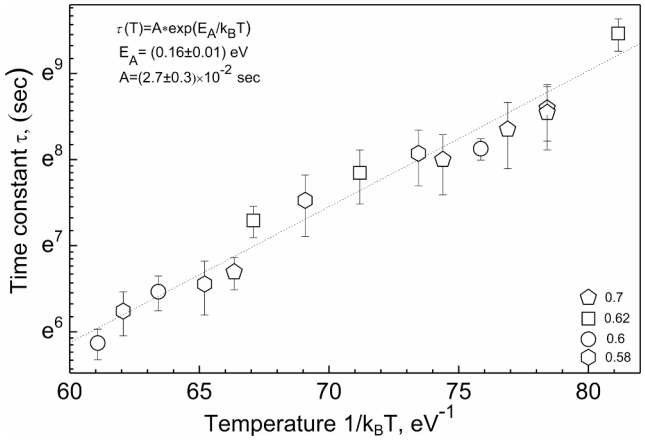

Fig. 4. Arrhenius plot $\tau(T) = A*\exp(E_A/k_BT)$ of the dependence of the exponential decay time constant τ on the annealing temperature $1/k_BT$ (open symbols) and its linear approximation (dotted line). Different symbols relate to the hydrogenated silica glass samples with initially different hydrogen content. E_A is the activation energy, A is the time constant, and k_B is the Boltzmann constant.

Arrhenius plot

$$\tau(\mathrm{T}) = A \times \exp(E_A/k_BT) \quad (1)$$

where the activation energy E_A is (0.16 ± 0.01) eV and time constant A is (2.7 ± 0.3) × 10^{-2} sec.

It is interesting to compare the obtained magnitude of the activation energy of hydrogen desorption with that of hydrogen diffusion through the silica glass. As shown earlier, the diffusion of hydrogen through the walls of a silica glass ampoule increases with temperature, showing also the activation-type behavior [22–24]. The activation energy of hydrogen diffusion obtained in these experiments varies from 0.37 eV to 0.43 eV in early publications [22,23] to 0.54 eV in the later work [24]. Some difference between these data may be related, in part, with possibly different compositions of the silica glass of the ampoules used. Nevertheless, the activation energy of hydrogen diffusion is at least two times higher than that of hydrogen desorption. Thus, in the temperature range under study, hydrogen diffusion from the bulk of the sample is relatively slower than hydrogen desorption from the sample surface. The difference between them results in depletion of the surface of the hydrogenated silica glass under annealing, which can be monitored by Raman spectroscopy. Using Eq. (1), the thermal stability of the hydrogenated silica glass can be characterized as follows: hydrogen content on the surface of the hydrogenated silica glass decreases by a thousand times in 170 years at liquid nitrogen temperature and in 1.5 min at room temperature. These estimates do not take into account possible changes in the activation energy of hydrogen desorption at a low hydrogen concentration.

In conclusion, hydrogen is dissolved in silica glass in the form of H_2 molecules. In the Raman spectra of the hydrogenated silica glass, the frequencies and relative intensities of the phonon bands of the silica glass matrix slightly change together with the appearance of new peaks of the rotational and stretching vibration modes of molecular hydrogen. The frequencies and bandwidths of the hydrogen phonon modes vary with the concentration of dissolved H_2 molecules in the silica glass. They differ from those of gaseous hydrogen because of considerable broadening and a multidirectional shift. Annealing of the hydrogenated silica glass samples at temperatures from 143 to 190 K results in the partial desorption of hydrogen and a concomitant exponential decrease in the intensity of the hydrogen rotational modes in the Raman spectra. The dependence of the exponential decay time constant τ on temperature T is well described by the Arrhenius formula $\tau(T) = A*\exp(E_A/k_BT)$ with the activation energy $E_A = (0.16 \pm 0.01)\ eV$ and time constant $A = (2.7 \pm 0.3) \times 10^{-2}$ sec. The obtained numerical data assume that hydrogen content in silica glass hydride falls in half within ~17 years at liquid nitrogen temperature and within 10 s under ambient conditions. Finally, rather low activation energy of hydrogen desorption indicates a weak van der Waals-type interaction between the dissolved hydrogen molecules and silica glass matrix.

CRediT authorship contribution statement

K.P. Meletov: Conceptualization, Investigation, Visualization, Writing – original draft, Writing – review & editing. **V.S. Efimchenko:** Resources, Methodology, Investigation, Writing – original draft.

Declaration of Competing Interest

The authors declare that they have no known competing financial interests or personal relationships that could have appeared to influence the work reported in this paper.

Acknowledgments

The authors are grateful to Dr. V. E. Antonov for discussions. This work is carried out within the state task of ISSP RAS.

References

[1] V.A. Yartys, M.V. Lototskyy, E. Akiba, R. Albert, V.E. Antonov, J.R. Ares, M. Baricco, N. Bourgeois, C.E. Buckle, et al., Magnesium based materials for hydrogen based energy storage: Past, present and future, Int. J. Hydrogen Energy 44 (2019) 7809–7859, https://doi.org/10.1016/j.ijhhydene.2018.12.212.
[2] K.P. Meletov, A.A. Maksimov, I.I. Tartakovskii, I.O. Bashkin, V.V. Shestakov, A. V. Krestinin, Y.M. Shulga, K. Andrikopoulos, Y. Arvanitidis, D. Christifilos, G. A. Kourouklis, Raman study of the high-pressure hydrogenated SWNT: in search of chemically bonded and adsorbed molecular hydrogen, Chem. Phys. Lett. 433 (2007) 335–339, https://doi.org/10.1016/j.cplett.2006.11.072.
[3] A. Timothy, T.A. Strobel, E.D. Sloan, C.A. Koh, A. Huq, A.J. Schultz, Molecular Hydrogen Occupancy in Binary THF−H_2 Clathrate Hydrates by High Resolution Neutron Diffraction, J. Phys. Chem. B 110 (2006) 14024–14027, https://doi.org/10.1021/jp063164w.
[4] K.A. Lokshin, Y. Zhao, Yusheng Zhao, Fast synthesis method and phase diagram of hydrogen clathrate hydrate, Appl. Phys. Lett. 88 (13) (2006) 131909, https://doi.org/10.1063/1.2190273.
[5] D.J. Durbin, C. Malardier-Jugroot, Review of hydrogen storage techniques for on board vehicle applications, Int. J. Hydrogen Energy 38 (2013) 14595–14617, https://doi.org/10.1016/j.ijhhydene.2013.07.-58.
[6] P. Jena, Materials for hydrogen storage: past, present, and future, J. Phys. Chem. Lett. 2 (3) (2011) 206–211, https://doi.org/10.1021/jz1015372.
[7] C.M. Hartwig, Raman scattering from hydrogen and deuterium dissolved in silica as a function of pressure, J. Appl. Phys. 47 (3) (1976) 956–959, https://doi.org/10.1063/1.322686.
[8] V.S. Efimchenko, V.K. Fedotov, M.A. Kuzovnikov, A.S. Zhuravlev, B.M. Bulychev, Hydrogen solubility in amorphous silica at pressures up to 75 kbar, J. Phys. Chem. B 117 (1) (2013) 422–425, https://doi.org/10.1021/jp309991x.
[9] V.S. Efimchenko, V.K. Fedotov, M.A. Kuzovnikov, K.P. Meletov, B.M. Bulychev, Hydrogen Solubility in Cristobalite at High Pressure, J. Phys. Chem. A 118 (44) (2014) 10268–10272, https://doi.org/10.1021/jp509470q.
[10] V.S. Efimchenko, N.V. Barkovskii, V.K. Fedotov, K.P. Meletov, Hydrogen solubility in amorphous Mg0.6SiO2.6 at high pressure, JETP 124 (6) (2017) 914–919, https://doi.org/10.1134/S1063776117050028.
[11] V.S. Efimchenko, N.V. Barkovskii, V.K. Fedotov, K.P. Meletov, S.V. Simonov, S. S. Khasanov, K.I. Khyapin, High-pressure solid solutions of molecular hydrogen in amorphous magnesium silicates, J. Alloy. Compd. 770 (2019) 229–235, https://doi.org/10.1016/j.jallcom.2018.08.111.
[12] V.S. Efimchenko, N.V. Barkovskii, V.K. Fedotov, K.P. Meletov, V.M. Chernyak, K. I. Khyapin, Destruction of fayalite and formation of iron and iron hydride at high hydrogen pressures, Phys. Chem. Min. 46 (2019) 743–749, https://doi.org/10.1007/s00269-019-01035-z.
[13] K.P. Meletov, V.S. Efimchenko, Raman study of hydrogen-saturated silica glass, Int. J. Hydrogen Energy 46 (2021) 24501–24509, https://doi.org/10.1016/j.ijhhydene.2021.04.144.
[14] L.G. Khvostantsev, V.N. Slesarev, V.V. Brazhkin, Toroid type high-pressure device: history and prospects, High Press. Res. 24 (3) (2004) 371–383, https://doi.org/10.1080/08957950412331298761.
[15] V.E. Antonov, I.O. Bashkin, S.S. Khasanov, A.P. Moravsky, Y.G. Morozov, Y. M. Shulga, Y.A. Ossipyan, E.G. Ponyatovsky, Magnetic ordering in hydrofullerite $C_{60}H_{24}$, J. Alloy. Compd. 330–332 (2002) 365–368, https://doi.org/10.1016/S0925-8388(01)01534-1.
[16] V.E. Antonov, B.M. Bulychev, V.K. Fedotov, D.I. Kapustin, V.I. Kulakov, I.A. Sholin, NH_3BH_3 as an internal hydrogen source for high pressure experiments, Int. J. Hydrogen Energy 42 (35) (2017) 22454–22459, https://doi.org/10.1016/j.ijhydene.2017.03.121.
[17] I.O. Bashkin, V.E. Antonov, A.V. Bazhenov, I.K. Bdikin, D.N. Borisenko, E. P. Krinichnaya, A.P. Moravsky, A.I. Harkunov, Y.M. Shul'ga, Y.A. Ossipyan, E. G. Ponyatovsky, Thermally stable hydrogen compounds obtained under high pressure on the basis of carbon nanotubes and nanofibers, JETP Lett. 79 (5) (2004) 226–230, https://doi.org/10.1134/1.1753421.
[18] K.P. Meletov, A nitrogen cryostat with adjustable temperature and cold loading of samples for the measurement of optical spectra, Instruments and Experimental, Techniques. 63 (2) (2020) 291–293, https://doi.org/10.1134/S0020441220020013.
[19] A. Chrissanthopoulos, N. Bouropoulos, S.N. Yannopoulos, Vibrational spectroscopic and computational studies of sol-gel derived CaO-MgO-SiO_2 binary and ternary bioactive glasses, Vib. Spectrosc. 48 (1) (2008) 118–125, https://doi.org/10.1016/j.vibspec.2007.11.008.
[20] E.J. Allin, T. Feldman, H.L. Welsh, Raman spectra of liquid and solid hydrogen, J. Chem. Phys. 24 (1956) 1116–1117, https://doi.org/10.1063/1. 1742711.
[21] T.A. Strobel, E.D. Sloan, C.A. Koh, Raman spectroscopic studies of hydrogen clathrate hydrates, J. Chem. Phys. 130 (2009), https://doi.org/10.1063/1.3046678, 014506-1-014506-10.
[22] R.W. Lee, R.C. Frank, D.E. Swets, Diffusion of hydrogen and deuterium in fused quartz, J. Chem. Phys. 36 (4) (1962) 1062–1071, https://doi.org/10.1063/1.1732632.
[23] J.E. Shelby, Molecular diffusion and solubility of hydrogen isotopes in vitreous silica, J. Appl. Phys. 48 (8) (1977) 3387–3394, https://doi.org/10.1063/1.324180.
[24] L. Shang, I.-M. Chou, W. La, R.C. Burruss, Y. Zhang, Determination of diffusion coefficients of hydrogen in fused silica between 296 and 523 K by Raman spectroscopy and application of fused silica capillaries in studying redox reactions, Geochim. Cosmochim. Acta 73 (2009) 5435–5443, https://doi.org/10.1016/j.gca.2009.0.